ORNL
MASTER COPY

ORNL-3674
UC-25 – Metals, Ceramics, and Materials
TID-4500 (31st ed.)

# CONTAMINATION OF REFRACTORY METALS BY RESIDUAL GASES IN VACUUMS BELOW $10^{-6}$ TORR

H. Inouye

OAK RIDGE NATIONAL LABORATORY
operated by
UNION CARBIDE CORPORATION
for the
U.S. ATOMIC ENERGY COMMISSION

Printed in USA. Price: $0.75 Available from the
Office of Technical Services
U. S. Department of Commerce
Washington 25, D. C.

LEGAL NOTICE

This report was prepared as an account of Government sponsored work. Neither the United States, nor the Commission, nor any person acting on behalf of the Commission:

A. Makes any warranty or representation, expressed or implied, with respect to the accuracy, completeness, or usefulness of the information contained in this report, or that the use of any information, apparatus, method, or process disclosed in this report may not infringe privately owned rights; or

B. Assumes any liabilities with respect to the use of, or for damages resulting from the use of any information, apparatus, method, or process disclosed in this report.

As used in the above, "person acting on behalf of the Commission" includes any employee or contractor of the Commission, or employee of such contractor, to the extent that such employee or contractor of the Commission, or employee of such contractor prepares, disseminates, or provides access to, any information pursuant to his employment or contract with the Commission, or his employment with such contractor.

ORNL-3674

Contract No. W-7405-eng-26

METALS AND CERAMICS DIVISION

# CONTAMINATION OF REFRACTORY METALS BY RESIDUAL GASES IN VACUUMS BELOW $10^{-6}$ TORR

H. Inouye

SEPTEMBER 1964

OAK RIDGE NATIONAL LABORATORY
Oak Ridge, Tennessee
operated by
UNION CARBIDE CORPORATION
for the
U.S. ATOMIC ENERGY COMMISSION

# CONTAMINATION OF REFRACTORY METALS BY RESIDUAL GASES IN VACUUMS BELOW $10^{-6}$ TORR

H. Inouye

## ABSTRACT

The contamination of niobium, molybdenum, tantalum, Nb–1% Zr, FS-85, D-43, Cb-752, TZM, and T-111 resulting from their extended exposure to the residual gases in high vacuums was measured by chemical analyses. This contamination was characterized in terms of the system pressure, metal temperature, exposure time, metal surface-to-volume ratio, and alloy composition. A second phase of the study was concerned with developing techniques for lowering the contamination of Nb–1% Zr with refractory metal envelopes, vapor-plated molybdenum, and intentional additions of nitrogen or $CH_4$ to vacuum atmosphere to counteract the noxious gases.

The residual gases in the vacuum system operating at pressures between $10^{-6}$ and $10^{-8}$ torr were mainly hydrogen, $H_2O$, CO, $CH_4$, nitrogen, and $CO_2$. The oxidizing gases at these pressures caused significant amounts of oxygen contamination of the above alloys when heated for 1000 hr between 600 to 1200°C. Although carburization also occurred, a competing carbon-oxygen reaction became important at the higher temperatures and caused decarburization of some of the alloys. The presence of titanium, zirconium, and hafnium in the above alloys promoted oxygen contamination while additions of tungsten and tantalum had no influence. Hydrogen and nitrogen contamination was not a problem.

Refractory metal envelopes effectively stabilized the carbon content of Nb-1% Zr but were erratic in their ability to lower the oxygen contamination. Molybdenum deposits $< 5 \times 10^{-5}$ in. thick produced by the reduction of $MoCl_5$ provided complete protection of the alloy up to 1062°C. Low concentrations of $CH_4$ added to the residual gases in the vacuum system lowered the oxygen contamination of TZM and niobium.

It was concluded that the contamination of refractory metals was controlled by four test variables: pressure, temperature, time, and sample thickness. For the temperature range investigated, the maximum permissible pressures are estimated to be near $10^{-9}$ torr for thin metal sections exposed for extended periods. Through the additional use of secondary control measures, such as metal barriers, metal surface deposits, and gas additions to the residual gases, the permissible atmospheres for niobium and tantalum alloys could be expanded to higher impurity concentrations and environments of inert gases. Furthermore, the present results indicate that it may be feasible to control the interstitial content of the alloys during heat treatment with suitable gas additions.

## INTRODUCTION

The interstitial elements, oxygen, carbon, nitrogen, and hydrogen, in refractory metals are now accepted as important constituents influencing their mechanical properties. Significant advances in the technology of controlling interstitials have been made in connection with melting and fabrication while concern over interstitial control during extended service at elevated temperature has not been emphasized until recently.

Currently, high vacuums are used to protect refractory metals at elevated temperature; however, the tendency for these metals to be contaminated by the residual gases in vacuum systems is well known by investigators in the field. Beyond this observation, the variables which influence the extent of contamination have not been documented.

It was the purpose of this investigation to measure the extent of gaseous contamination of several alloys of interest resulting from their extended exposure to vacuums below $10^{-6}$ torr and to characterize this contamination in terms of the alloy composition and the test

conditions. A second objective was concerned with exploring techniques for controlling contamination by interstitials.

This report presents the results of a study of the contamination characteristics of molybdenum, TZM (Mo–0.5% Ti–0.07% Zr), niobium, Nb–1% Zr, D-43 (Nb–10% W–1% Zr–0.1% C), Cb-752 (Nb–10% W–2.5% Zr), FS-85 (Nb–27% Ta–10% W–1% Zr), tantalum, and T-111 (Ta–8% W–2% Hf) in the range 600 to 1200°C, pressures of $10^{-6}$ to $10^{-8}$ torr, and test times up to 1000 hr. Data are also presented on the influence of foil wraps, vapor-plated molybdenum, and intentional low-pressure gas additions on controlling the contamination of molybdenum, TZM, niobium, tantalum, and Nb–1% Zr.

## EXPERIMENTAL PROCEDURE

The method used to measure contamination was chemical analyses. Specimen weight changes were also determined to indicate whether bulk transfer (e.g., evaporation) of species other than the gases had occurred. Both hardness and mechanical property changes were considered to be unreliable due to the known aging tendencies of refractory metals and also undesirable because the measurements were incapable of identifying the specific contaminants.

The test apparatus consisted of a 2 1/4-in.-diam porcelain tube which was heated by a resistance furnace. Vacuum and access ports of pyrex were fused to the open ends of the porcelain tube. The system was cold trapped with liquid nitrogen and pumped by a 25 liter/sec glass oil diffusion pump, backed up by a 15 liter/sec metal diffusion pump and a mechanical pump. Following system bakeouts with flexible heater tapes, pressures of $5 \times 10^{-8}$ torr could be attained at 1200°C during a run.

Mechanically polished sheet specimens, 1/2 × 3/4 in. and up to 0.040 in. thick, were wired with tantalum to a 1 1/2-in.-diam inner porcelain tube which was perforated with four rows of 1/4-in.-diam holes at 1-in. intervals along its 18-in. length. To minimize the temperature gradient of a specimen, each specimen was wired to the holder with its 1/2-in. dimension in the direction of the tube axis.

The specimen holder was then positioned in the furnace tube such that the specimen location in the natural temperature gradient of the furnace was known within 1/8 in. Temperatures were measured with a travelling Pt vs Pt-10% Rh thermocouple in a porcelain thermocouple protection tube which extended throughout the length of the hot zone on its axial center line. This design permitted the testing of up to 64 specimens between 600 to 1200°C in a single run.

System pressures were measured with a RG-75 Veeco ionization gage at least twice daily. When it was desired to maintain a pressure higher than the minimum for the system, the pumping speed was reduced by lowering the power input to the diffusion pumps. When an intentional gas addition was required, it was bled into the system through a high vacuum valve. The reported test pressures were computed by dividing the sum of the instantaneous pressure times the time interval between readings by the total exposure time.

The composition of the residual gases in the vacuum system was determined by adsorption on Linde 13X zeolite or activated charcoal at −195°C, releasing the gases by heating to 300°C into a pyrex ampoule with proper valving, then analyzing the sample with a mass spectrometer. For the system pressures investigated, gas collection periods of about 200 hr gave sample pressures between 0.2 to 1.0 torr.

## RESULTS AND DISCUSSION

### Part 1. Contamination Characteristics of Refractory Metals

#### Composition of the Residual Gases

The compositions of the residual gases in the system containing 20 Nb-1% Zr specimens between 600 to 1200°C and pressures of $1.0 \times 10^{-5}$, $1.0 \times 10^{-6}$, and $3.0 \times 10^{-7}$ torr are shown in Table 1. These analyses show that the major components were hydrogen, $H_2O$, and nitrogen plus CO. The larger difference noted in the hydrogen and the hydrocarbon contents in the analysis for gases at $3 \times 10^{-7}$ torr compared to those for pressures of $10^{-5}$ and $10^{-6}$ torr was probably a reflection of the difference in the adsorbing abilities of activated charcoal and zeolite.

Table 1. Composition of Residual Gases in a Vacuum System

| Gas Species | Composition (vol %) | | | Average |
|---|---|---|---|---|
| | $1 \times 10^{-5}$[a] (torr) | $1 \times 10^{-6}$[a] (torr) | $3 \times 10^{-7}$[b] (torr) | |
| Hydrogen | 44 | 61 | 4.8 | 37 |
| $CH_4$ | 4.4 | 0.2 | 3.1 | 2.6 |
| $H_2O$ | 18.0 | 7.3 | 13.7 | 13 |
| Hydrocarbon | 6.2 | 5.1 | 36.5 | 16 |
| Nitrogen plus CO | 21.4 | 24 | 34 | 26 |
| Oxygen | 1.0 | 0.16 | 0.8 | 0.65 |
| $CO_2$ | 5.0 | 2.2 | 4.8 | 4.0 |

[a]Residual gases adsorbed on activated charcoal at −195°C.

[b]Residual gases adsorbed on Linde 13X zeolite at −195°C.

These analyses were considered to be only approximations due to the sampling method used and were not carried out in all the tests for this reason.

Assuming that these analyses were representative of the test atmosphere, it is seen that the residual gases could cause oxygen, nitrogen, hydrogen, and carbon contamination of the alloys.

## Effect of the Metal Surface-to-Volume Ratio

The sorption of the residual gases by the heated metal specimens may be controlled by the kinetics of the sorption and diffusion processes or by the attainment of equilibrium between the gases and the metal if given sufficient time. If contamination is governed by reaction kinetics, the extent of contamination would be dependent on the metal surface-to-volume ratio. If gas-metal equilibria describe the situation after extended exposure, then the extent of contamination would be independent of the surface-to-volume ratio.

Letting $\Delta C$ represent the increase in the concentration of the gas in the metal of volume, V, and surface area, A, and assuming non-equilibrium conditions (i.e., the kinetically controlled case):

$$\Delta C \sim A/V \sim 1/X \quad . \tag{1}$$

For metal thicknesses of $X_1$ and $X_2$ (the thickness, X, is assumed to be << width and length; therefore X = thickness of a sheet or thin-walled tube), the corresponding values of $\Delta C_1$ and $\Delta C_2$ are related by Eq. (2):

$$\frac{\Delta C_1}{\Delta C_2} = \frac{X_2}{X_1} \quad . \tag{2}$$

The measured contamination of specimens of Nb-1% Zr ranging in thickness from 0.020 to 0.040 in. expressed as percent increase, contamination ratio, and by weight per unit of area are tabulated in Table 2. An examination of the data clearly shows that $\Delta C$ depended on $A/V \sim 1/X$ (surface-to-volume ratio) and that equilibrium was not attained for times approaching 1000 hr.

In order to compare the extent of contamination of refractory metals for the various test conditions employed, it was necessary to express the contamination on a unit of area (e.g., $mg/cm^2$) basis or, if expressed on a weight basis (e.g., ppm), to normalize the data to equal metal thicknesses. In this study the chemistry changes in the specimens in weight percent were converted to milligrams per centimeters squared from a knowledge of the specimen areas and weights. The contamination if expressed on a weight basis (ppm) was computed by dividing the specific weight change ($mg/cm^2$) by the weight of metal having the dimensions $1 \times 1 \times 0.1$ cm thick. The normalized data, therefore, represent the contamination from one side of a metal specimen 0.1 cm (0.0394 in.) thick.

To account for the deposition and/or evaporation of material other than the gaseous contaminants, the contamination was measured by weight changes as well as by chemistry changes. As shown in Table 3, these

Table 2. The Effect of the Specimen Thickness on the Contamination of Nb–1% Zr[a]

| Test Temp (°C) | Specimen Thickness (in.) | | Contamination[b] (wt %) | | Ratio | | Weight Increase ($mg/cm^2$) | |
|---|---|---|---|---|---|---|---|---|
| | $X_1$ | $X_2$ | $\Delta C_1$ | $\Delta C_2$ | $X_2/X_1$ | $\Delta C_1/\Delta C_2$ | $X_1$ | $X_2$ |
| 856 | 0.0201 | 0.0391 | 0.0724 | 0.0378 | 1.94 | 1.91 | 0.138 | 0.132 |
| 988 | 0.0200 | 0.0308 | 0.0966 | 0.0646 | 1.54 | 1.50 | 0.185 | 0.183 |
| 1081 | 0.0200 | 0.0384 | 0.1396 | 0.0696 | 1.92 | 2.01 | 0.266 | 0.243 |
| 1135 | 0.0198 | 0.0393 | 0.1506 | 0.0766 | 1.98 | 1.97 | 0.292 | 0.274 |
| 1201 | 0.0197 | 0.0382 | 0.2464 | 0.1354 | 1.94 | 1.72 | 0.540 | 0.552 |

[a]984 hr at $5.6 \times 10^{-7}$ torr.

[b]Sum of oxygen, carbon, and nitrogen contamination.

Table 3. A Comparison of the Contamination of Nb–1% Zr by Weight Change and by Chemical Analysis[a]

| Test Temperature (°C) | By Weight Change (ppm) | By Chemical Analysis (ppm) |
|---|---|---|
| 578 | –21 | 15 |
| 744 | 40 | 58 |
| 896 | 40 | 105 |
| 1009 | 195 | 192 |
| 1130 | 252 | 254 |
| 1182 | 482 | 287 |
| 1190 | 492 | 404 |

[a]1000 hr at $2.7 \times 10^{-7}$ torr.

effects were negligible since weight changes appeared to be mainly due to interstitial changes. The data contained in this report are based on chemical analyses normalized as described above. When the specimen thickness is given, the contamination on a weight basis is from both sides.

Effect of Alloy Composition and Temperature

A comparison of the total chemistry change of Nb–1% Zr, niobium, tantalum, and molybdenum resulting from their exposure to the residual gases for 1000 hr at $2.7 \times 10^{-7}$ torr is made in Fig. 1. Up to about 600°C, contamination was negligible for all compositions. Above 600°C the differences in the reactivity of these metals became apparent and were observed to decrease in the order Nb–1% Zr, niobium, tantalum, and molybdenum.

The contribution of the specific contaminants to the total contamination of Nb–1% Zr is shown in Fig. 2. In this test, oxygen contamination accounted for over 80% of the total, while carbon contamination essentially accounted for the balance. Table 4 compares the chemistry changes in molybdenum, tantalum, and niobium under the same conditions and shows that molybdenum was purified while oxygen was the principal contaminant of tantalum and niobium.

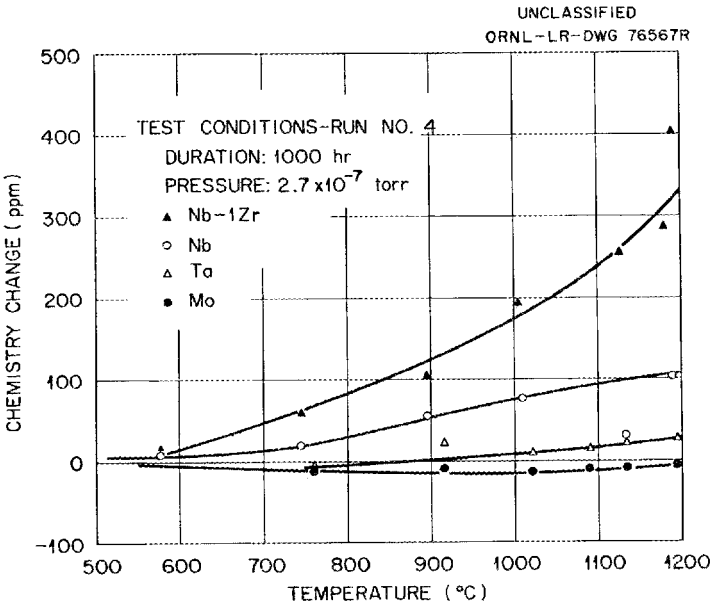


Fig. 1. Contamination of Nb–1% Zr, Niobium, Tantalum, and Molybdenum at $2.7 \times 10^{-7}$ torr.

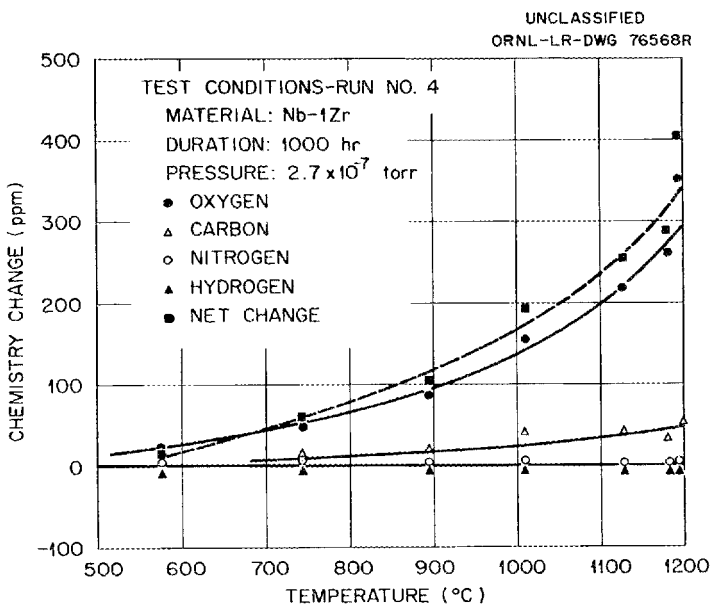


Fig. 2. Contamination of Nb–1% Zr by Oxygen, Carbon, Hydrogen, and Nitrogen at $2.7 \times 10^{-7}$ torr.

Table 4. The Contamination of Molybdenum, Tantalum, and Niobium by Residual Gases in 1000 hr at $2.7 \times 10^{-7}$ torr

| Temperature (°C) | Chemistry Change[a,b] (ppm) | | |
|---|---|---|---|
| | ΔO | ΔN | ΔC |
| Molybdenum | | | |
| 757 | −66 | < −1 | −4 |
| 916 | −8 | < −1 | −4 |
| 1023 | −10 | < −1 | −6 |
| 1088 | −9 | < −1 | −2 |
| 1133 | −7 | < −1 | −5 |
| 1195 | −2 | < −1 | −6 |
| Tantalum | | | |
| 757 | −7 | < −1 | −2 |
| 916 | 7 | < −1 | 17 |
| 1023 | 14 | 0 | −5 |
| 1088 | 13 | −1 | −3 |
| 1133 | 14 | −3 | −13 |
| 1195 | 29 | −1 | −1 |
| Niobium | | | |
| 578 | 12 | ~1 | −4 |
| 744 | 16 | ~1 | 0 |
| 896 | 39 | ~1 | 15 |
| 1009 | 62 | ~1 | 12 |
| 1130 | 35 | ~1 | 0 |
| 1190 | 93 | ~1 | 8 |

[a]Data normalized, actual chemistry change between 2.5 to 4 times above values.

[b]ΔH was approximately −1 ppm.

The significant increase in the reactivity of Nb-1% Zr by a factor of about 3 over unalloyed niobium was undoubtedly due to the zirconium in the alloy. To further clarify the influence of zirconium on the reactivity of niobium alloys, binary niobium-zirconium alloys containing 0.62, 1.03, and 2.63 wt % Zr were tested. The oxygen contamination in these alloys resulting from an exposure of 501 hr at $1.0 \times 10^{-6}$ torr did not show a clear dependence on the zirconium content according to the data presented in Table 5. These results indicate that as little as 0.6 wt % Zr is sufficient to markedly increase the reactivity of niobium alloys.

The contamination characteristics of the more complex alloys are indicated in Tables 6 and 7. The purification of molybdenum in high vacuums was confirmed, as shown in Table 6, while TZM was contaminated with oxygen at all temperatures. An abrupt increase in the oxygen contamination from 60 ppm to over 300 ppm occurred in TZM between 1100 to 1200°C. This contamination was confirmed by the brittle behavior of the alloy in bend tests at room temperature. The increased susceptibility of TZM for oxygen contamination was concluded to be due to the titanium and zirconium in the alloy. Examination of the data on TZM will clearly show that decarburization increased in severity with the oxygen contamination. This aspect of contamination will be discussed in Part 2 of this report.

The oxygen contaminations resulting from a 902-hr exposure of the advanced tantalum and niobium alloys at an average pressure of $7.2 \times 10^{-8}$ torr are compared in Table 7. The rather wide range of contamination between the alloys when expressed as "parts per million" was mainly due to the density variations of the alloys. A more accurate and representative comparison can be made using the weight change data (computed from the analysis) which is independent of the alloy density. With a few exceptions, there appear to be no significant differences in the reactivity of these alloys on this basis.

Table 5. The Effect of Zirconium Content on the Oxygen Contamination of Niobium-Zirconium Alloys

| Test Temperature (°C) | Contamination ($mg/cm^2$) | | |
|---|---|---|---|
| | 0.62% Zr | 1.03% Zr | 2.63% Zr |
| 761 | 0.0202 | 0.035 | 0.048 |
| 929 | 0.0287 | 0.050 | 0.079 |
| 1053 | 0.0254 | 0.072 | 0.059 |
| 1133 | 0.0860 | 0.127 | 0.068 |
| 1172 | 0.128 | 0.136 | 0.070 |
| 1197 | 0.143 | 0.170 | 0.162 |
| 1205 | 0.230 | 0.258 | 0.183 |

[a]Test conditions: 501 hr at $1.0 \times 10^{-6}$ torr.

Table 6. The Contamination of 0.020-in. Molybdenum and TZM Sheet in 1000 hr at $2.4 \times 10^{-7}$ torr

| Temperature (°C) | Interstitial Content | | Change in Interstitials | |
|---|---|---|---|---|
| | Oxygen (ppm) | Carbon (ppm) | ΔO (ppm) | ΔC (ppm) |
| Molybdenum | | | | |
| control | 77 | 50 | --- | --- |
| 914 | 61 | 20 | −16 | −30 |
| 1032 | 49 | 20 | −28 | −30 |
| 1109 | 60 | 70 | −17 | +20 |
| 1181 | 86 | 20 | +9 | −30 |
| 1196 | 68 | 20 | −9 | −30 |
| TZM | | | | |
| control | 10 | 180 | --- | --- |
| 740 | 51 | 240 | 41 | 60 |
| 914 | 48 | 210 | 38 | 30 |
| 1032 | 65 | 150 | 55 | −30 |
| 1109 | 62 | 90 | 52 | −90 |
| 1193 | 330 | 60 | 320 | −120 |
| 1196 | 350 | 40 | 340 | −140 |

Table 7. Oxygen Contamination of Niobium and Tantalum Alloys After 902 hr at $7.2 \times 10^{-8}$ torr

| Test Temperature (°C) | Nb–1% Zr | T-111 | FS-85 | Cb-752 | D-43 |
|---|---|---|---|---|---|
| Weight Increase ($mg/cm^2$) | | | | | |
| 964 | --- | --- | 0.036 | --- | --- |
| 1018 | 0.082 | 0.026 | --- | 0.062 | 0.053 |
| 1129 | 0.099 | 0.060 | 0.076 | 0.093 | 0.120 |
| 1187 | --- | --- | --- | 0.286 | --- |
| 1195 | 0.146 | 0.132 | 0.151 | --- | 0.137 |
| Oxygen Increase[a] (ppm) | | | | | |
| 964 | --- | --- | 34 | --- | --- |
| 1018 | 95 | 15 | --- | 69 | 58 |
| 1129 | 115 | 36 | 71 | 103 | 132 |
| 1187 | --- | -- | --- | 317 | --- |
| 1195 | 171 | 79 | 142 | --- | 150 |

[a]Normalized; densities of alloys used in calculation: Nb–1% Zr – 8.57; T-111 – 16.7; FS-85 – 10.6; Cb-752 – 9.02; D-43 – 9.08.

In comparing the oxygen contamination between Nb–1% Zr and D-43 and between FS-85 and D-43, it was concluded that 10 wt % W and 27 wt % Ta in niobium have little, if any, effect on the reactivity of the alloys. By comparing the contamination in D-43 with Cb-752, it is suggested that increasing the zirconium content from 1 to 2.5% significantly increases the oxygen contamination – an effect that was not observed for the binary niobium-zirconium alloys. This apparent anomalous behavior might be related to the influence of the test pressure ($1 \times 10^{-6}$ vs $7 \times 10^{-8}$ torr); however, the data are limited and more tests would be required to show this. The oxygen contamination of T-111 was consistently lower than the niobium alloys, suggesting that hafnium in tantalum is less reactive than zirconium in niobium. Further experimentation is required to prove this point.

Effect of Time and Pressure

From the kinetic theory of gases, the mass of gas, G, incident upon a unit of surface area per unit time is given by Eq. (3).

$$G = 5.833 \times 10^{-2}\ P(M/T)^{1/2}\ \mathrm{g/cm^2 \cdot sec} \quad . \tag{3}$$

The increase in the concentration, $\Delta C$, of this gas in a metal due to its sorption by the metal is:

$$\Delta C = \frac{\alpha G A t}{V \rho} = \frac{\alpha G t}{X \rho}\ \mathrm{g/g} \tag{4}$$

or more conveniently for a sheet of metal or tube contaminated from one side

$$\Delta C = \frac{82.5\ \alpha P (M/T)^{1/2}\ t}{X \rho} \times 10^6\ \mathrm{ppm} \tag{5}$$

where

P = gas pressure (torr),
M = molecular weight of the gas (g),
A = area exposed to the gas ($cm^2$),
t = exposure (hr),
X = specimen thickness (in.),
$\alpha$ = sticking probability,
$\rho$ = alloy density ($g/cm^3$),
V = volume of metal ($cm^3$),
and
T = temperature (°K).

For a specific metal exposed to a particular gas and temperature, Eq. (5) reduces to:

$$\Delta C = \frac{kPt}{X} \text{ ppm} \tag{6}$$

where k is a constant having the dimensions ppm·in./torr-hr and could be considered to be proportional to the reaction rate constant for the metal.

The dependence of $\Delta C$ on $1/X$ has been demonstrated by the data in Table 2. To check the dependence of $\Delta C$ on P and t, the contamination of Nb–1% Zr at four pressure-time levels was determined and the data are summarized in Table 8. By examination, it is apparent that $\Delta C$ was not a function of the pressure-time product.

If the contamination was assumed to depend on $t(P)^{1/2}$, the contamination ratios should be in the proportions 50:52:74:93. The actual ratios averaged out to be 32:52:78:99. This may be fortuitous; however, the dependence of $\Delta C$ on $t(P)^{1/2}$ is a remarkable resemblance to Sievert's gas solubility law, $C = S(P)^{1/2}$, where S is the solubility limit.

The data in Table 8 can be approximated by the empirical expression

$$\Delta C = \frac{kt(P)^{1/2}}{X} \quad . \tag{7}$$

The average values of k calculated from the data increased exponentially with temperature according to the curves shown in Figs. 3 and 4. The appropriate expressions for the contamination of Nb–1% Zr as a function of temperature, pressure, and time can be expressed by either of the two equations listed below, depending on the temperature.

$$\Delta C \ (750\text{–}1000\,^{\circ}\text{C}) = \frac{90.6\ t(P)^{1/2} \exp - 5500/RT}{X} \tag{8}$$

or

$$\Delta C \ (1000\text{–}1200\,^{\circ}\text{C}) = \frac{6.89 \times 10^{4}\ t(P)^{1/2} \exp - 22{,}400/RT}{X} \tag{9}$$

where

$\Delta C$ = increase in oxygen concentration (ppm),
t = exposure (hr),
P = system pressure (torr),
X = thickness (in.), and
T = absolute temperature.

Table 8. Effects of Exposure Time and Pressure on the Contamination of Nb–1% Zr

| Temp (°C) | Total Contamination (ppm)[a] | | | | Contamination Ratio |
|---|---|---|---|---|---|
| | $t(P)^{1/2} = 0.50$[b] | $t(P)^{1/2} = 0.52$[c] | $t(P)^{1/2} = 0.74$[d] | $t(P)^{1/2} = 0.93$[e] | |
| 800 | 55 | 83 | 132 | 172 | 34:52:83:108 |
| 900 | 65 | 107 | 160 | 207 | 32:52:77:100 |
| 1000 | 85 | 147 | 214 | 272 | 30:52:76:96 |
| 1050 | 103 | 180 | 260 | 330 | 30:52:75:95 |
| 1100 | 128 | 225 | 330 | 418 | 30:52:76:97 |
| 1150 | 166 | 300 | 450 | 567 | 29:52:78:98 |
| 1200 | 224 | 405 | 650 | 800 | 29:52:83:103 |
| | | | Average | | 32:52:78:99 |

[a]Normalized.

[b]501 hr at $1.0 \times 10^{-6}$ torr.

[c]1000 hr at $2.7 \times 10^{-7}$ torr.

[d]984 hr at $5.6 \times 10^{-7}$ torr.

[e]932 hr at $1.0 \times 10^{-6}$ torr.

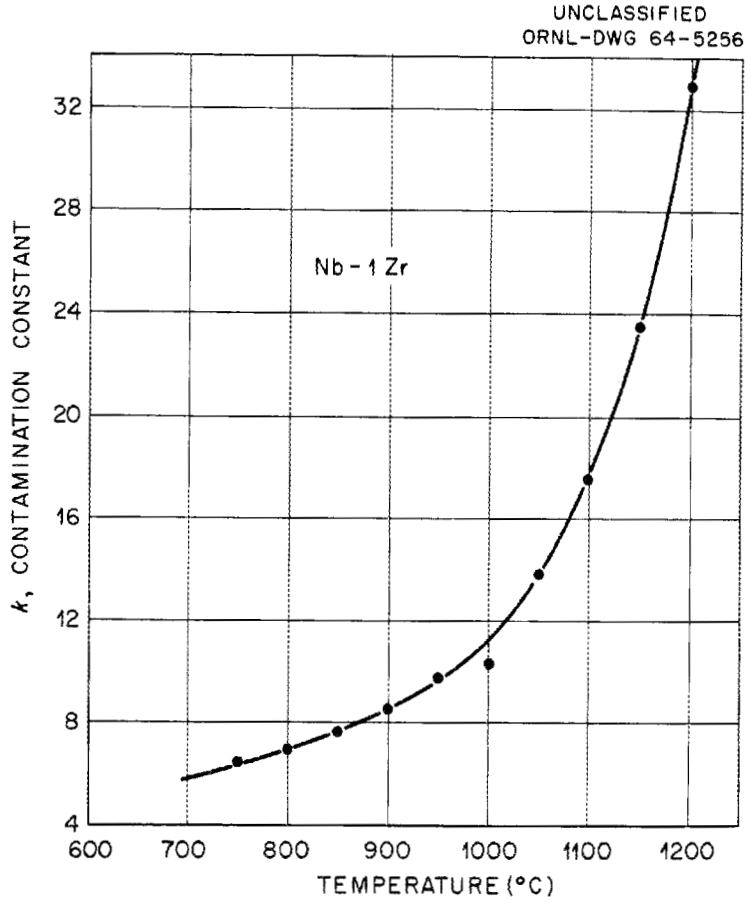


Fig. 3. Dependence of Contamination Rate of Nb–1% Zr on Temperature.

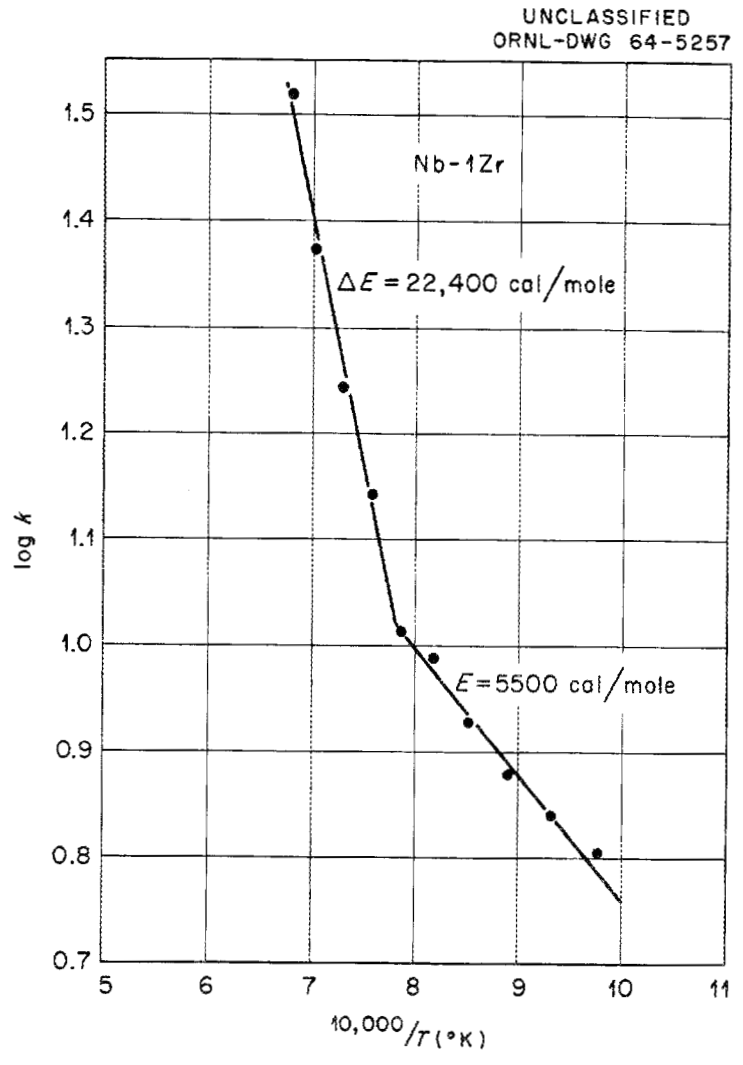


Fig. 4. Variation of the Contamination Rate of Nb–1% Zr with the Absolute Temperature.

The expressions for Eqs. (8) and (9) are applicable to the contamination of tubing or sheet from one side only. For contamination from both sides, the half-thickness should be used.

## Part 2. Contamination Control

There are at least three methods by which the contamination of refractory metals by the residual gases can be controlled in a specific test (thickness and exposure fixed). The most obvious method is to reduce the residual gas pressure by the proper design of the vacuum system. It is expected, however, that conditions may arise where the necessary low pressures cannot be attained or are not desirable for other reasons.

A second method, which might accomplish the same end result as high vacuums, is to wrap the metal to be protected with a thin refractory metal envelope. When this technique becomes impractical due to geometric complexities, vapor-plated metal coatings that are compatible with the substrate metal may be beneficial.

The third method depends upon the neutralization of the noxious residual gases by the addition of selected gases at low pressures. The purpose of the gas additions would be to cause their preferential sorption on the metal surface or to combine with the deleterious gases to form a gaseous reaction product which is pumped from the vacuum system. Exploratory experiments on the last two methods were conducted and showed some interesting possibilities, as will be discussed below.

### Influence of Refractory Metal Barriers on the Contamination of Nb–1% Zr

It was considered that metal envelopes surrounding the metal to be protected would serve as a getter for the gaseous contaminants and/or as a physical barrier. If the main function of the metal envelope was to absorb the contaminants, the efficiency (in terms of reducing contamination) of the various metal foils would be expected to increase with their reactivity. If, however, the sticking probabilities of the

gases on the foils are low, their effectiveness would increase as the conductance (leaks) of the envelope decreased. In the latter case, the protective ability of the envelope would be relatively independent of the type of barrier used.

The influence of foil wraps of molybdenum, tantalum, and Nb–1% Zr on reducing the contamination of Nb–1% Zr at $2.7 \times 10^{-7}$ torr is shown in Fig. 5. This test showed that foil wraps significantly reduced the contamination above 600°C and became more effective as the temperature increased. The preferred envelope metal appears to be molybdenum, followed by tantalum, then Nb–1% Zr. The order of efficiency was in the reverse order of their reactivity (see Fig. 1).

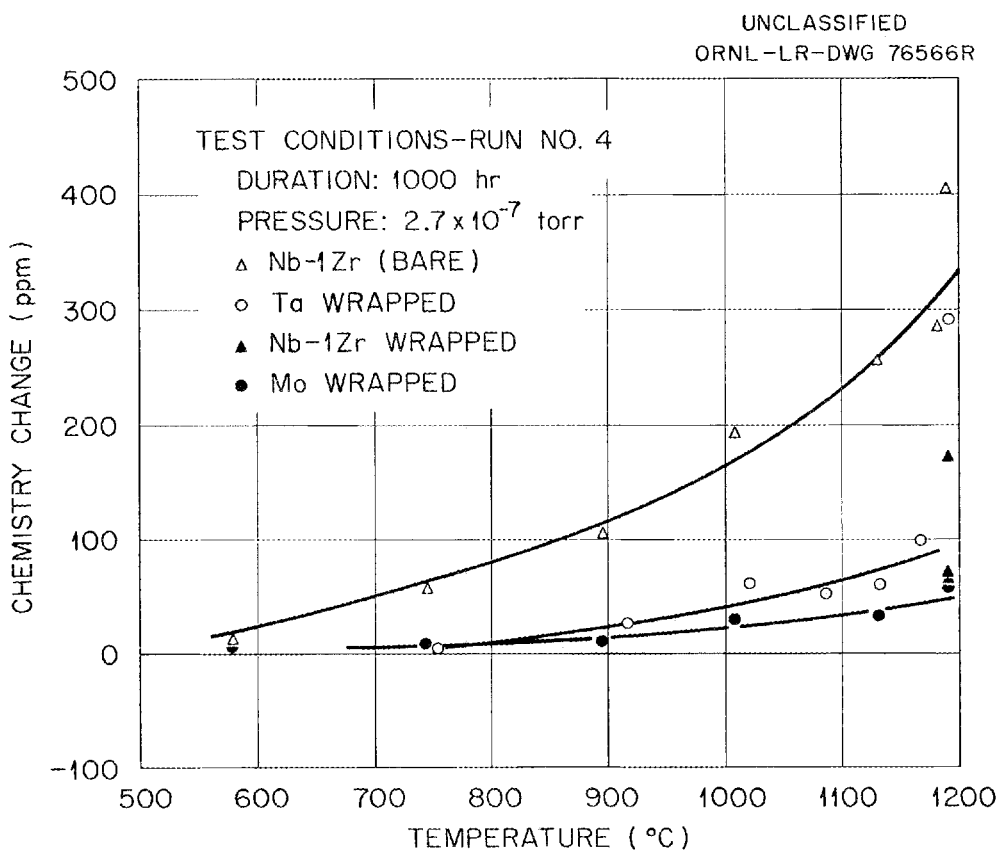


Fig. 5. Influence of Foil Wraps on Reducing the Contamination of Nb–1% Zr at $2.7 \times 10^{-7}$ torr.

Since it appeared that foil wraps were barriers rather than sinks for the residual gases, care was taken to duplicate the wrapping procedure in subsequent tests. The foil dimensions in the latter experiments provided for an overlap of one specimen width in one direction, while a fold of 1/8 in. was made at the narrow ends.

The test results at $1.0 \times 10^{-6}$ torr shown in Table 9 were obtained for foil thicknesses as follows: Nb–1% Zr – 0.005 in.; molybdenum – 0.003 in.; tantalum – 0.003 in.; and tungsten – 0.005 in. Based on the chemistry changes, the foil wraps effectively eliminated carbon contamination, were erratic in the reduction of the oxygen contamination which ranged from a factor of 2 to 98, and appeared to be of minor benefit in lowering the nitrogen contamination.

Table 9. The Effect of Foil Wraps on the Contamination of Nb–1% Zr at $1 \times 10^{-6}$ torr and 1000 hr[a]

| Temp (°C) | Control | Type of Foil | | | |
|---|---|---|---|---|---|
| | | Mo | Ta | W | Nb–1% Zr |
| | | ΔC (ppm) | | | |
| 734–770 | 25 | –30 | –5 | 0 | –30 |
| 902–936 | 60 | –30 | –10 | –20 | --- |
| 1029–1045 | 265 | –15 | –20 | –10 | –30 |
| 1109–1113 | --- | –30 | --- | –5 | –25 |
| 1150–1176 | 215 | –20 | –20 | --- | +30 |
| 1189–1202 | 90 | –10 | –10 | –15 | –10 |
| | | ΔO (ppm) | | | |
| 724–770 | 200 | 25 | 45 | 65 | 55 |
| 902–936 | 490 | 25 | 65 | 60 | --- |
| 1029–1045 | 455 | 30 | 65 | 90 | 55 |
| 1109–1113 | --- | 70 | --- | 85 | 65 |
| 1150–1176 | 980 | 10 | 240 | --- | 55 |
| 1189–1202 | 1280 | 155 | 640 | 135 | 105 |
| | | ΔN (ppm) | | | |
| 724–770 | 1 | 5 | –5 | 14 | 2 |
| 902–936 | 1 | 13 | 3 | 14 | --- |
| 1029–1045 | 10 | 10 | 7 | 16 | 8 |
| 1109–1113 | --- | 15 | --- | 6 | 6 |
| 1150–1176 | 25 | --- | 10 | --- | 26 |
| 1189–1202 | 33 | 13 | 10 | 10 | 24 |

[a]Contamination based on 0.040-in. sheet (both sides). Starting analysis: 1.03 wt % Zr, 80 ppm C, 120 ppm O, and 67 ppm N.

Although the superiority of one metal foil over another was not clearly indicated by the present tests, it was concluded that the primary function of the envelope was to act as a barrier for the residual gases in the vacuum system. Because of the wide difference in the reactivity of the foils evaluated, one must further conclude that the sticking probabilities are small numbers. Fortunately, this characteristic is an economic advantage because the least costly metal would perform as efficiently as the more expensive metals.

When reliability is desired through the use of a protective layer, the inconsistent performance of metal envelopes would be a distinct drawback. The required reliability can better be attained with vapor-plated metals because such coatings characteristically result in total coverage due to their high throwing power.

To demonstrate feasibility, molybdenum was vapor plated from $MoCl_5$ onto Nb–1% Zr specimens which were subsequently exposed to the residual gases in the vacuum system. Vapor-plated molybdenum deposits calculated from the weight increase of the test specimen to be about $3 \times 10^{-6}$ in. thick were obtained at a $MoCl_5$ plating pressure of $2 \times 10^{-5}$ torr for 20 hr at 950°C. Complete protection of Nb–1% Zr by this thickness of molybdenum was obtained below 750°C in a 500-hr test at $4 \times 10^{-7}$ torr.

By plating molybdenum at a $MoCl_5$ pressure of $5 \times 10^{-4}$ torr plus $1.2 \times 10^{-3}$ torr hydrogen to aid in the reduction of the compound, plating thicknesses between 2 to $5 \times 10^{-5}$ in. thick were obtained after a 20-hr plating run and decomposition temperatures between 800 to 900°C. For this thickness of molybdenum, complete protection of Nb–1% Zr up to temperatures of 1062°C was observed for an exposure of 1000 hr at $9.4 \times 10^{-7}$ torr, as shown in Table 10.

These encouraging results were based upon the change in the chemistry of the specimens due to their exposure to the vacuum atmosphere and do not include the oxygen contamination resulting from the volatile impurities in the $MoCl_5$ powder.

It is postulated that the increase in the oxygen contamination at the higher test temperatures results from deterioration of the deposit due to the inward diffusion of the molybdenum into Nb–1% Zr. Because

Table 10. The Effect of Vapor-Plated Molybdenum on the Contamination of Nb–1% Zr[a]

| Test Temperature (°C) | Thickness of Molybdenum (mil) | Molybdenum-Plated | | Control | |
|---|---|---|---|---|---|
| | | ΔO (ppm) | ΔC (ppm) | ΔO (ppm) | ΔC (ppm) |
| 966 | 0.019 | –30 | none | 320 | –20 |
| 1062 | 0.044 | –70 | –10 | 580 | 20 |
| 1117 | 0.038 | 130 | 10 | 880 | 40 |
| 1151 | 0.048 | 330 | –20 | 1180 | 40 |
| 1163 | 0.029 | 980 | 50 | 1180 | 50 |

[a]0.040-in. sheet exposed 1000 hr at $9.4 \times 10^{-7}$ torr.

the integrity of the protective coating depends upon its thickness, greater protection at the higher temperatures would be expected if the plating thickness was increased. As an indication of the thickness required, Ogilvie and Moll[1] have shown that within 0.0011 in. the composition of a molybdenum-niobium diffusion couple changes from 100% Mo to 100% Nb after 1728 hr at 1300°C. It is expected, therefore, that a vapor-plated molybdenum deposit approximately 0.001 in. thick would afford complete protection of Nb–1% Zr at 1200°C for 1000 hr.

## Influence of Nitrogen on the Contamination of Refractory Metals

The oxidation rates of niobium in air at $5 \times 10^{-4}$ torr are about one tenth the rate in oxygen at $1 \times 10^{-4}$ torr as shown in Figs. 6 and 7. The nitrogen contamination in the air tests above was about 1% of the oxygen contamination. Since visible reaction layers did not form during the earlier stages of the test, these results were thought to be due to a chemisorbed nitrogen layer which inhibited the oxidation rate of the alloy.

Because the contamination data presented in Part 1 of this report showed that nitrogen contamination was slight or did not occur at the pressures investigated, it appeared that oxygen contamination might be

[1]R. E. Ogilvie and S. H. Moll, Research to Determine the Composition of Dispersed Phases in Refractory Metal Alloys, AMR-1536 (Aug. 1963).

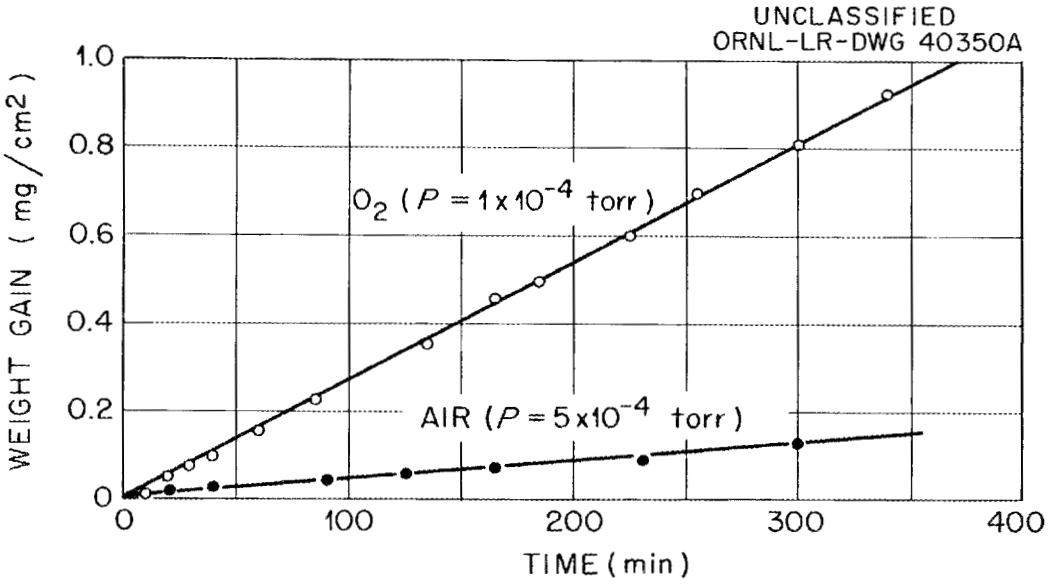


Fig. 6. Contamination of Niobium at 1000°C.

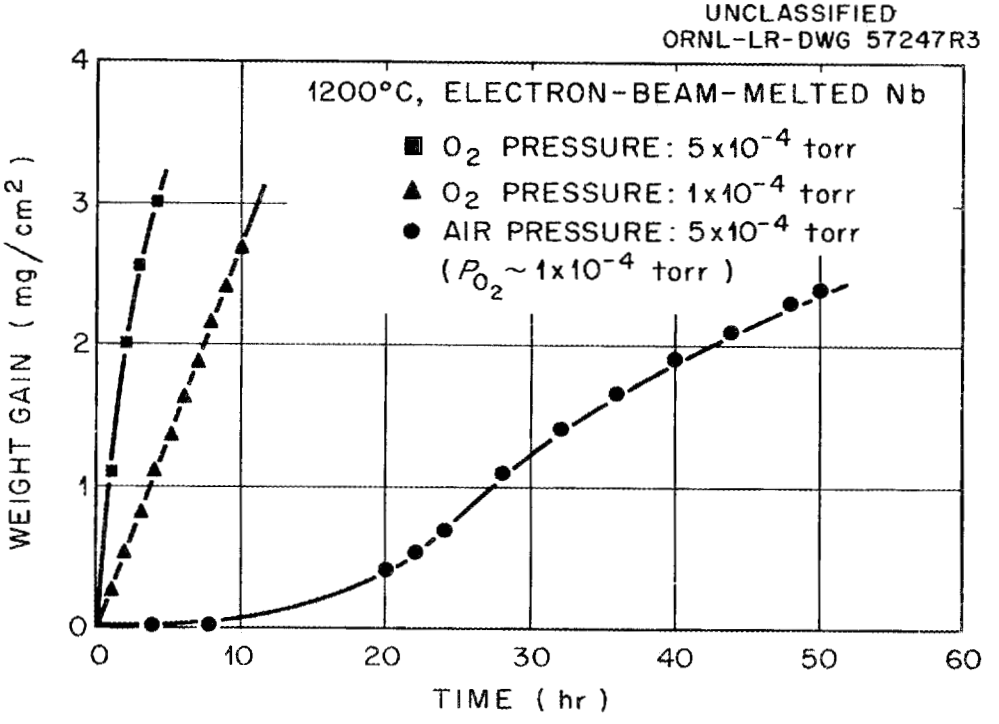


Fig. 7. Contamination of Niobium at 1200°C.

reduced with a nitrogen overpressure at a slight risk of nitrogen contamination. To determine whether the $10^{-4}$ torr data could be extrapolated to lower pressures, specimens of Nb–1% Zr, TZM, niobium, molybdenum, and tantalum were exposed for 1000 hr to the residual gases in a system with a base pressure of $2.4 \times 10^{-7}$ torr plus a nitrogen overpressure of $6.6 \times 10^{-7}$ torr.

The oxygen contamination of Nb–1% Zr, niobium, and tantalum, resulting from the exposure to the above atmosphere, is shown in Table 11. A comparison of these data with those shown in Tables 3 and 4 clearly indicated that the intentional nitrogen addition to the residual gas atmosphere did not function as intended. Similarly, the oxygen contamination of molybdenum and TZM was unaffected by the presence of this concentration of nitrogen.

Table 12 lists the nitrogen contamination in Nb–1% Zr, niobium, and tantalum due to the nitrogen overpressure. It was observed that the extent of nitrogen contamination of Nb–1% Zr was about equal to niobium at the higher temperatures. In addition, neither molybdenum nor TZM was contaminated with nitrogen in this test. These results show that zirconium and/or titanium do not promote the affinity of these alloys for nitrogen as they do for oxygen contamination.

Approximate nitrogen sticking probabilities ($\alpha$) for Nb–1% Zr, niobium, and tantalum were calculated from the nitrogen contamination and the nitrogen overpressure to be those in Table 12. Generally, these data show that $\alpha$ values are low and increase with temperature except in the case of tantalum where $\alpha$ appeared to be insensitive to temperature.

## Influence of $CH_4$ on the Contamination of Refractory Metals

At high temperatures, the carbon in metals will react with oxygen to form CO as a reaction product. Because the end point of this reaction is the equilibrium concentrations of carbon and oxygen, the element which is in excess will remove the other. As an example, serious decarburization occurred in TZM when it became contaminated with oxygen (Table 6).

Table 11. Oxygen Contamination of Nb–1% Zr, Niobium, and Tantalum in 1000 hr at a Base Pressure of $2.4 \times 10^{-7}$ torr Plus $6.6 \times 10^{-7}$ torr Nitrogen

| Test Temperature (°C) | Oxygen Increase (ppm) | | |
|---|---|---|---|
| | Nb–1% Zr | Niobium | Tantalum |
| 618 | 19 | -- | |
| 780 | 47 | 19 | 21 |
| 934 | 94 | 53 | 35 |
| 1040 | 187 | 64 | 25 |
| 1113 | 268 | -- | 19 |
| 1154 | 361 | -- | |
| 1155 | 378 | 69 | |
| 1178 | 408 | -- | 36 |
| 1191 | 465 | 107 | |
| 1198 | 495 | -- | |
| 1202 | 519 | 164 | 74 |

Table 12. Nitrogen Contamination of Nb–1% Zr, Niobium, and Tantalum in 1000 hr at a Base Pressure of $2.4 \times 10^{-7}$ torr Plus $6.6 \times 10^{-7}$ torr Nitrogen

| Test Temperature (°C) | Nitrogen Increase (ppm) | | | Sticking Probability ($\alpha$) | | |
|---|---|---|---|---|---|---|
| | Nb–1% Zr | Nb | Ta | Nb–1% Zr | Nb | Ta |
| | | | | $\times 10^{-4}$ | | |
| 618 | 5 | -- | -- | 0.92 | -- | -- |
| 780 | 4 | 4 | 6 | 0.71 | 0.75 | 2.5 |
| 934 | 7 | 4 | 7 | 1.5 | 0.84 | 2.8 |
| 1040 | 23 | 9 | 4 | 4.7 | 1.81 | 1.4 |
| 1113 | 28 | -- | 5 | 5.6 | -- | 1.7 |
| 1154 | 33 | -- | -- | 6.6 | -- | -- |
| 1155 | 43 | 45 | -- | 8.6 | 9.0 | -- |
| 1178 | 40 | -- | 4 | 8.0 | -- | 1.4 |
| 1191 | 48 | 45 | -- | 9.6 | 9.0 | -- |
| 1198 | 55 | 56 | -- | 11.0 | 11.0 | -- |
| 1202 | 53 | -- | 6 | 11.0 | -- | 2.2 |

In theory, it is possible to remove oxygen from metals or control the oxygen contamination by providing a source of carbon. In those alloys that depend on carbon for high-temperature strength, decarburization may also be controlled by the neutralizing influence of a carburizing gas.

It is apparent from the above statements that the control of the carbon-oxygen reaction may be a necessity in the heat treatment and testing of carbide-strengthened alloys such as D-43, TZM, T-222, TZC, and similar alloys. The problem becomes especially acute in the heat treatment of thin gage sheet because of the surface-to-volume effect discussed previously. The feasibility of controlling oxygen contamination and decarburization with $CH_4$ was therefore determined.

Specimens of TZM, Nb–1% Zr, and niobium were tested in a vacuum system at a base pressure of $1.9 \times 10^{-7}$ torr to which a $CH_4$ overpressure of $6.3 \times 10^{-7}$ torr was introduced. The influence of $CH_4$ on the oxidation and decarburization of TZM, Nb–1% Zr, and niobium is shown in Figs. 8, 9, and 10, respectively. In the case of TZM, $CH_4$ effectively eliminated oxygen contamination up to about 1100°C. Above this temperature, oxygen contamination occurred but was about one third of that measured for an equivalent test in the absence of $CH_4$. With respect to the decarburization of TZM, this concentration of $CH_4$ was apparently too low to prevent it. At all temperatures, the TZM specimens treated in $CH_4$ could be bent through several 90° bend reversals at room temperature without fracture. Under the same test conditions, the oxygen contamination of niobium was reduced but with Nb–1% Zr the improvement was marginal. Surprisingly, the data on the carbon analyses suggested that $CH_4$ lowered the carbon contamination.

## CONCLUSIONS

The residual gases in a high-vacuum system at pressures between $10^{-6}$ and $10^{-8}$ torr are mainly hydrogen, $H_2O$, CO, $CH_4$, $CO_2$, and nitrogen. The $H_2O$, CO, and $CO_2$ caused significant amounts of oxygen contamination in refractory metal alloys when heated between 600 and 1200°C for periods of 1000 hr. Although carburization was also observed, a competing

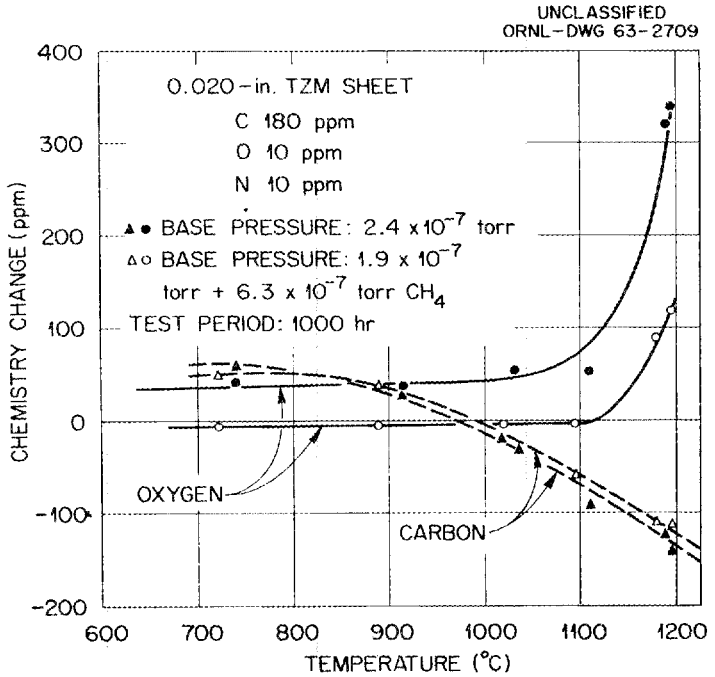


Fig. 8. Effect of $CH_4$ on the Oxygen and Carbon Contamination of TZM.

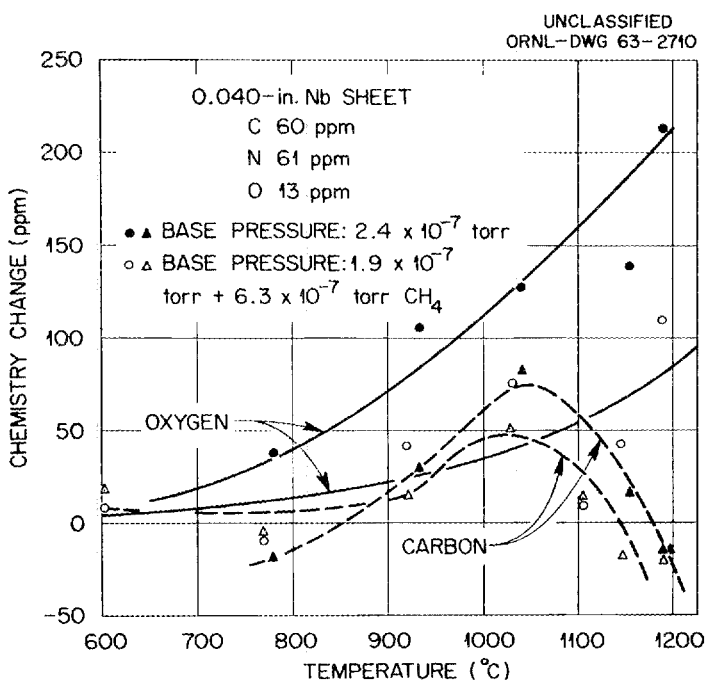


Fig. 9. Effect of $CH_4$ on the Oxygen and Carbon Contamination of Niobium.

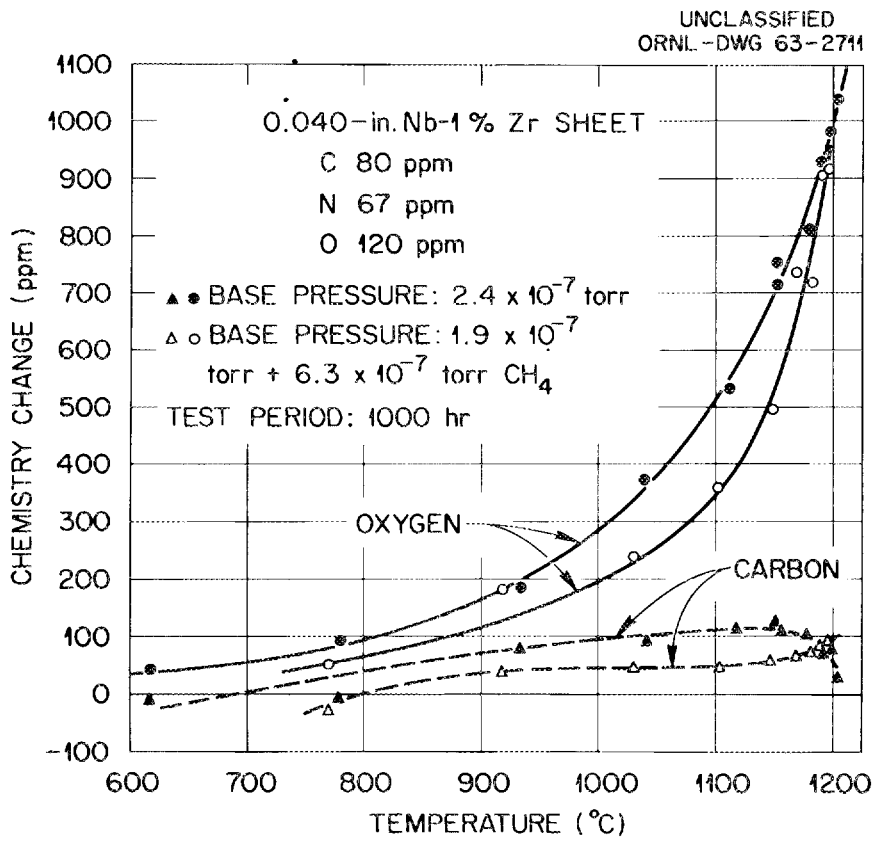


Fig. 10. Effect of $CH_4$ on the Oxygen and Carbon Contamination of Nb–1% Zr.

carbon-oxygen interaction became significant at the higher temperatures and caused severe decarburization in alloys depending on carbon for strength. Hydrogen contamination was not encountered while nitrogen contamination was negligible.

Alloying elements such as titanium, zirconium, and hafnium, which form oxides thermodynamically more stable than the base metals niobium, tantalum, and molybdenum, promoted oxygen contamination. Zirconium and titanium did not influence the nitrogen contamination. Tungsten additions apparently had no effect on the contamination of niobium or tantalum alloys.

A more detailed study of the contamination characteristics of Nb–1% Zr showed that the extent of oxygen contamination was largely

governed by the system pressure, temperature, exposure time, and the metal surface-to-volume ratio. These variables are related to each other by the expressions:

$$\Delta C\ (750\text{–}1000\,^{\circ}C) = \frac{90.6\ t(P)^{1/2}\ \exp - 5500/RT}{X}$$

or

$$\Delta C\ (1000\text{–}1200\,^{\circ}C) = \frac{6.89 \times 10^{4}\ t(P)^{1/2}\ \exp - 22{,}400/RT}{X}$$

where

$\Delta C$ = increase in oxygen concentration due to contamination from one side (ppm),

$t$ = exposure time (hr),

$P$ = system pressure (torr), and

$X$ = specimen thickness (in.).

In addition to the above controlling variables, it was determined that wrapping the alloy with refractory metal envelopes, such as molybdenum, tantalum, tungsten, and Nb–1% Zr, provided for an effective method of stabilizing the carbon content of the alloy as well as lowering the oxygen contamination. Because the effectiveness of the refractory metal envelopes in lowering the oxygen contamination was erratic and appeared to be independent of the type of metal used, it was concluded that the sticking probabilities of the residual gases on molybdenum, tantalum, tungsten, and Nb–1% Zr were low. Under these conditions, the principal function of the envelopes was to serve as a physical barrier to gas flow toward the metal to be protected. Preliminary experiments indicate that a very thin layer of vapor-plated molybdenum on Nb–1% Zr provides complete protection from the residual gases in vacuum systems at least to 1050 °C for 1000 hr.

Intentional low-pressure gas additions of nitrogen to the residual gases did not lower the oxygen contamination as hoped. On the other hand, $CH_4$ at $6 \times 10^{-7}$ torr effectively lowered the oxygen contamination of TZM and niobium but was less effective for Nb–1% Zr. The present experiments indicated that higher $CH_4$ pressures are desirable and may also be effective in preventing decarburization in alloys like D-43, T-222, and TZM.

## Recommendations

The metallurgy of refractory metals ultimately becomes concerned with problems associated with the influence of the interstitials oxygen, carbon, nitrogen, and hydrogen. Complete documentation of the alloy properties under a variety of conditions cannot be made unless their high-vacuum stability, solubility limits, phases which they form, their diffusion rates, and the gas-metal reaction kinetics are known. Because the alloys of current interest are not independent of the above factors, it is recommended that future investigations be directed toward obtaining such information.

It is the opinion of the author that it is especially important to establish the carbon stability in high vacuums because many existing alloys and those being developed depend upon its presence for strength. Because carbon stability is directly related to oxygen contamination, a fruitful area of study lies in the determination of the carbon-oxygen equilibria for carbide-strengthened alloys.

Along the same lines, establishment of the $H_2$-$CH_4$-C relationships in these alloys would be invaluable in controlling the carbon content in all stages of heat treatment as well as during extended service times. The tendency toward decarburization in high vacuums may not become negligible until pressures are reduced to the range $10^{-9}$ torr.

Although unambiguous quantitative data do not exist, it is suspected that there is only one condition of temperature and pressure at which the interstitials are in equilibrium with the atmosphere. At any other condition, degassing or contamination occurs and migration of the interstitials is a distinct possibility in a temperature gradient. In this respect, thin layers of molybdenum or tungsten merit special consideration because the total chemical character of the alloy can be altered by such an adherent layer and may function as effective barriers toward interstitial migration. It is further reasoned that such layers due to their inert character may expand the permissible atmosphere for niobium and tantalum alloys to the inert gases and reducing atmospheres.

## ACKNOWLEDGMENTS

The main conclusions of this report relied entirely on the results of the chemical analyses. Because the analyses were in complete accord with the expected behavior of the various alloys, it is a strong argument in favor of their accuracy. W. R. Laing and H. Davis of the Analytical Chemistry Division are to be commended for their excellent service.

ORNL-3674

UC-25 — Metals, Ceramics, and Materials
TID-4500 (31st ed.)

INTERNAL DISTRIBUTION

1–3. Central Research Library
4. Reactor Division Library
5–6. ORNL — Y-12 Technical Library
Document Reference Section
7–26. Laboratory Records Department
27. Laboratory Records, ORNL RC
28. ORNL Patent Office
29. R. J. Beaver
30. J. Burka
31. O. B. Cavin
32. E. L. Compere
33. R. S. Crouse
34. F. L. Culler
35. J. E. Cunningham
36. J. H. DeVan
37. R. G. Donnelly
38. S. T. Ewing
39. J. H Frye, Jr.
40. R. G. Gilliland
41. T. G. Godfrey
42. W. R. Grimes
43. J. P. Hammond
44. R. L. Heestand
45–49. M. R. Hill
50. D. O. Hobson
51. H. W. Hoffman
52–53. H. Inouye
54. T. Kollie
55. C. E. Larson
56. C. F. Leitten
57. A. P. Litman
58. T. S. Lundy
59. H. G. MacPherson
60. R. E. MacPherson, Jr.
61. H. E. McCoy
62. G. E. Moore
63. J. F. Murdock
64. R. E. Reed
65. T. K. Roche
66. R. G. Ross
67. H. W. Savage
68. C. E. Sessions
69. G. M. Slaughter
70. R. L. Stephenson
71. J. O. Stiegler
72. J. A. Swartout
73. W. C. Thurber
74. R. A. Vandermeer
75. A. M. Weinberg
76. J. A. Wheeler, Jr.
77–96. G. D. Whitman
97. R. P. Wichner
98. A. A. Burr (consultant)
99. J. R. Johnson (consultant)
100. C. S. Smith (consultant)
101. R. Smoluchowski (consultant)

EXTERNAL DISTRIBUTION

102. C. M. Adams, Jr., MIT
103. G. M. Anderson, AEC, Washington
104. C. H. Armbruster, AEC, Washington
105. D. E. Baker, GE, Hanford
106. B. B. Baschkin, Atomic Energy Document Center at the Gmelin Institute
107. R. T. Begley, Westinghouse Astronuclear Laboratory
108. John Bonchak, Universal-Cyclops
109. V. P. Calkins, GE, NMPO
110. S. S. Christopher, AEC, Washington
111. T. D. Cooper, Wright-Patterson AFB
112–113. D. F. Cope, AEC, ORO
114. J. W. R. Creagh, NASA, Lewis Research Center
115. D. W. Dayton, BMI

116. E. M. Douthett, AEC, Washington
117. R. B. Duffield, General Atomic Division, General Dynamics Corporation
118. Ersel Evans, GE, Hanford
119. T. E. Firle, General Atomic Division, General Dynamics Corporation
120. P. N. Flazella, GE, Cincinnati
121. D. C. Goldberg, Westinghouse Astronuclear Laboratory
122. J. L. Gregg, Cornell University
123. D. H. Gurinsky, BNL
124. R. Hall, Lewis Research Center
125. E. E. Hoffman, GE, Cincinnati
126. P. King, Atomics International
127. P. M. Mayfield, ANL
128. T. W. McIntosh, AEC, Washington
129. W. McNeish, Universal-Cyclops
130. C. E. Meyers, General Motors Research Laboratories
131. T. A. Moss, NASA, Lewis Research Center
132. R. A. Noland, ANL
133. R. G. Oehl, AEC, Washington
134. R. A. Pasternak, Stanford Research Institute
135. D. V. Ragone, General Atomic Division, General Dynamics Corporation
136. L. M. Raring, Pratt & Whitney, CANEL
137. Louis Rosenblum, NASA, Lewis Research Center
138. N. Saunders, NASA, Lewis Research Center
139. F. C. Schwenk, AEC, Washington
140. P. Shahinian, U. S. Naval Research Laboratory
141. J. Simmons, AEC, Washington
142. E. E. Stansbury, University of Tennessee
143. D. K. Stevens, AEC, Washington
144. C. O. Tarr, GE, Cincinnati
145. E. G. Thompson, Rocketdyne, Division of North American Aviation Corporation
146. L. Van Someren, Thermo Electron Engineering Corporation
147. G. W. Wensch, AEC, Washington
148. M. J. Whitman, AEC, Washington
149. A. Wronski, Union Carbide, European Research Associates, Belgium
150. Research and Development, ORO
151–726. Given distribution as shown in TID-4500 (31st ed.) under Metals, Ceramics, and Materials category (75 copies OTS)